ChemComm

COMMUNICATION

View Article Online
View Journal | View Issue

Cite this: *Chem. Commun.*, 2024, **60**, 14220

Received 25th September 2024,
Accepted 5th November 2024

DOI: 10.1039/d4cc04981k

rsc.li/chemcomm

Water-resistant boronic ester vitrimer with hydrophobic side chain protection†

Justin Jian Qiang Mah, [ab] Hongzhi Feng,[c] Nayli Erdeanna Binte Surat'man,[c] Bofan Li, [c] Sheng Wang *[c] and Zibiao Li *[acd]

A boronic ester vitrimer with high hydrolytic stability afforded by fluorinated side-chain protection is reported, withstanding high moisture and underwater environments with no performance degradation, which can also be self-healed, reprocessed and recycled, presenting a significant step towards the design of more robust and eco-friendly circular materials.

The increasing demand for sustainable materials has catalyzed significant research in the field of polymer chemistry, particularly focusing on the development of recyclable and reprocessable polymers. Traditional polymers, while versatile and widely used, pose significant environmental challenges due to their persistent nature and the difficulties associated with their disposal and recycling. To address these issues, materials designed for multiple lifecycles through efficient recycling and reprocessing dubbed circular polymers have emerged as a promising solution.[1] A critical aspect of designing such circular polymers is the incorporation of dynamic covalent reactions that allow bonds to exchange or be broken and reformed under specific conditions, enabling the construction of robust yet adaptable polymer networks. Current methods leveraging dynamic bonds in circular polymers primarily include polarized C=C double bonds,[2,3] imines,[4,5] disulfides,[6,7] boronic esters,[8–10] and Diels–Alder adducts.[11,12]

However, several dynamic covalent systems such as boronic esters and imines suffer from poor stability under ambient conditions, which hinders the range of applications of such materials.[13] Since these dynamic bonds are predominantly based on condensation reactions, the presence of moisture or protic solvents could possibly induce reverse reactions and thus degrade the material properties. For imine-based systems, intramolecular hydrogen bonding or post-synthetic conversion into more stable linkages such as aromatic imines, hydrazones, acyl hydrazones and oximes are readily available, significantly improving stability.[14,15] In contrast, methods to stabilize boronic ester systems are scarce, which has severely limited the use of this highly dynamic system in practical applications. Thus far, the most widely utilized method is to introduce B–N coordination bonds into the boronic ester network to form more stable 6-membered cyclic structures (Fig. S1a, ESI†), which was first reported by Zhang *et al.*[16] More recently, Kirchner *et al.* used a sterically-hindered *ortho*-substituting crosslinker to achieve a boronic ester cage that was stable in water (Fig. S1b, ESI†).[17] However, the inclusion of B–N coordination bonds and *ortho*-substituting boronic ester crosslinkers are not readily available, restricting this method to specific monomers that require multi-step synthesis and grafting.

To improve the practicality of materials containing the highly versatile boronic ester systems, the development of alternative methods to improve on the water-sensitivity of boronic ester materials is imperative. Previously, reports of using external hydrophobic additions or coatings such as hydrophobic plasticizers and hydrophobic finishing over poly(lactic acid) materials were able to provide a certain level of hydrolytic resistance to the material.[18,19] Intrigued by these attempts, we hypothesize that the inclusion of hydrophobic polymer side-chains considered as a protective mechanism would grant the material inherent hydrolytic stability. Hence, we report a boronic ester vitrimer with improved hydrolytic stability imparted by hydrophobic fluorinated side chains (Fig. S1c, ESI†).

[a] *Institute of Materials Research and Engineering (IMRE), Agency for Science, Technology and Research (A*STAR), 2, Fusionopolis Way, Innovis #08-03, Singapore 138634, Republic of Singapore. E-mail: lizb@imre.a-star.edu.sg*
[b] *Division of Chemistry and Biological Chemistry, School of Physical and Mathematical Sciences, Nanyang Technological University, Singapore 637371, Republic of Singapore*
[c] *Institute of Sustainability for Chemicals, Energy and Environment (ISCE2), Agency for Science, Technology and Research (A*STAR), 1 Pesek Road, Jurong Island, Singapore 627833, Republic of Singapore. E-mail: wang_sheng@isce2.a-star.edu.sg*
[d] *Department of Materials Science and Engineering, National University of Singapore, 9 Engineering Drive 1, Singapore 117576, Republic of Singapore*

† Electronic supplementary information (ESI) available: Materials, characterization methods, synthesis and experimental procedures, characterization data including ^{1}H NMR spectra, GPC trace, IR spectra, TGA thermograms, DSC thermograms, DMA curves, stress relaxation curves, stress–strain curves, digital photos of reprocessed and chemical recycled samples. See DOI: **https://doi.org/10.1039/d4cc04981k**

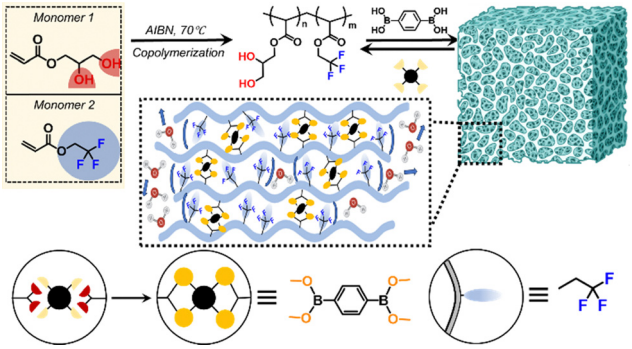

Fig. 1 Synthetic route of linear copolymer LP1 and illustration of dynamic crosslinking and hydrophobic protection afforded by fluorinated side chains in FV1.

A linear polymer was first synthesized from a vinyl diol monomer 2,3-dihydroxypropyl acrylate (DHPA, monomer 1) and fluorinated vinyl monomer 2,2,2-trifluoroethyl acrylate (TFA, monomer 2), which was copolymerized randomly under free-radical conditions with AIBN to obtain a copolymer (LP1) bearing 20% dihydroxy side chains for boronic ester linkages and 80% hydrophobic fluorinated side chains which were crosslinked to form the water-resistant boronic ester material by adding 1,4-phenylenebisboronic acid, leading to a 10% overall crosslinking degree (Fig. 1).

LP1 was characterized with ^{1}H nuclear magnetic resonance (^{1}H NMR) and Fourier-transform infrared spectroscopy (FTIR), confirming the inclusion of both the monomers in the linear polymer with the presence of the signals of both monomers in the FTIR and ^{1}H NMR spectrum in a ratio of 8 : 2, indicating the successful polymerization of LP1 (Fig. S2–S4, ESI†). The conversion of LP1 to FV1 was characterized with FTIR (Fig. S5, ESI†) to confirm the reaction of –OH in LP1 with 1,4-phenylenebisboronic acid forming the boronic ester, which was evident with the reduction of the 3300 cm^{-1} signal belonging to –OH (Fig. S6, ESI†) after half of the free –OH groups were used to form B–O–C in the boronic ester linkages. In addition, the signals corresponding to the B–O–H stretching and bending of 1,4-phenylenediboronic acid at 1340 cm^{-1} and 643 cm^{-1} respectively showed a clear shift to 1365 cm^{-1} and 660 cm^{-1} after crosslinking to form B–O–C in FV1 (Fig. S7, ESI†). To understand the distribution of BO and CF_3 moieties in FV1, scanning electron microscopy with energy dispersive X-ray spectroscopy (SEM-EDX) was conducted, revealing that the elements B/O and F are spread evenly throughout FV1, without being clustered together (Fig. S8, ESI†). Swelling and gel content analyses were also conducted for FV1 by immersing 0.2 g of FV1 samples in chloroform ($CHCl_3$), ethyl acetate (EA), diethyl ether (DE) and tetrahydrofuran (THF) for three days before the mass of the samples was taken before and after drying under vacuum. FV1 was able to swell significantly in EA (494%), THF (346%), and DE (287%), but comparatively less in $CHCl_3$ (118%). FV1 showed high gel contents in these solvents, with the lowest being 87% in DE, indicating the formation of a crosslinked network (Fig. S9, ESI†).

Based on thermogravimetric analysis (TGA) of FV1, the initial degradation temperature $T_{d5\%}$ (temperature at which 5% weight loss occurred) under a nitrogen atmosphere was determined to be 309 °C, indicating a good degree of thermal stability for FV1 (Fig. S10, ESI†). The glass transition temperature (T_g) of LP1 was determined to be −1.48 °C, which was increased to 14.3 °C after crosslinking with 1,4-phenylenediboronic acid, due to a decrease in mobility of the polymer network after crosslinking in FV1 (Fig. S11, ESI†). As the T_g of FV1 is well below room temperature, under ambient conditions, topology network rearrangement through boronic ester exchange is feasible, which allows the polymer network to facilitate self-healing. The storage modulus (E') curve of the FV1 (Fig. S12, ESI†) indicates that the materials follow a temperature-dependent viscoelastic behaviour with an E' of 2250 MPa in its glassy state (T_g −30 °C), which decreases to 1.27 MPa in its rubbery state (T_g +30 °C). Under a continuous applied strain of 10%, FV1 was able to relax to 1/e of the stress applied under 50 s at room temperature (Fig. S13, ESI†), demonstrating its ability to rapidly rearrange its topology network even at room temperature, which is optimal for self-healing and recycling purposes. By correlating the stress relaxation time with increasing temperatures (Fig. S14, ESI†), it was determined that stress relaxation of FV1 follows an Arrhenius relationship, with a determined activation energy (E_a) of 31.7 kJ mol^{-1}, which is in agreement with other reported materials with boronic ester linkages.[20] FV1 was also subjected to tensile testing at a rate of 30 mm min^{-1} with a Young's modulus of 34.8 MPa and achieved a maximum stress of 5.45 MPa and a maximum strain of 242% before breakage (Fig. S15, ESI†).

To evaluate the effects of the hydrophobic fluorinated side chains on the hydrolytic stability, a control non-fluorinated vitrimer sample (HV1) of similar molecular weight was prepared using the same procedures as FV1 while replacing 2,2,2-trifluoroethyl acrylate with ethyl acrylate (Fig. S16–S18, ESI†). DSC, DMA analysis, tensile tests and FTIR analysis were conducted to test the effects of the fluorinated side chains in the protection of the boronic ester linkages. Samples of FV1 and HV1 were left in an environment of 65% RH at 25 °C up to 7 days with the samples analysed *via* DSC after a 3- and 7-day period (Fig. S19 and S20, ESI†). The DSC curve and T_g of FV1 showed no appreciable changes after 7 days, demonstrating strong resilience in the high moisture environment, a higher humidity compared to what was observed in Zhang *et al.*'s work, conducted at 40% RH.[16] Surprisingly, a similar observation was made for HV1 with no appreciable changes in its DSC curve and only a slight drop of 2 °C in its T_g, indicating that a certain level of protection was present in HV1 as well, which can be attributed to the fact that –CH_3 side chains are also hydrophobic, albeit to a lesser extent when compared to –CF_3 side chains. However, when the FV1 and HV1 samples were immersed in water for 30 min (Fig. 2c and d), a clear shift of the DSC curve was observed for HV1 with a drop of 8 °C for its T_g, while FV1 showed no significant changes in the DSC curve and T_g, which demonstrated a greater degree of resilience for the boronic ester linkages in FV1. Similarly, when analysed with DMA (Fig. S21 and S22, ESI†), FV1 showed no appreciable changes to its T_g while the non-fluorinated vitrimer HV1 showed a visible drop in T_g of 10 °C. To understand the effects on its mechanical properties, tensile testing was

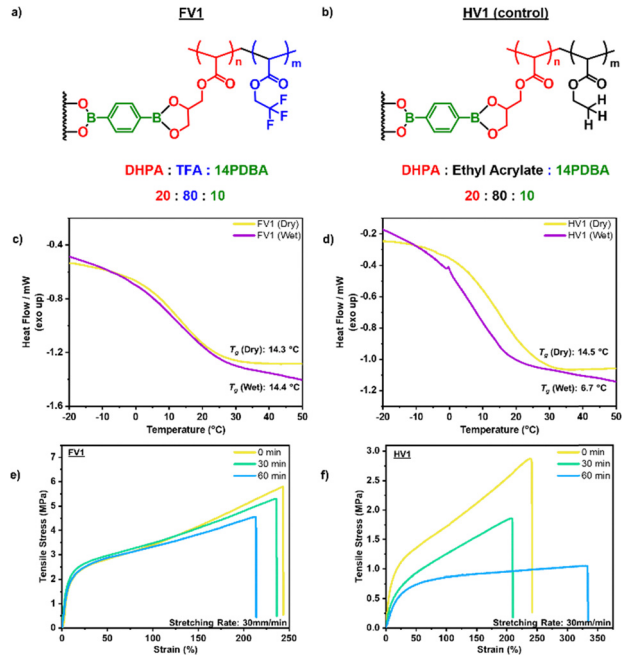

Fig. 2 Comparison of FV1 with the non-fluorinated counterpart. (a) Molecular structure of FV1 with monomer and crosslinker ratio; (b) molecular structure of HV1 with monomer and crosslinker ratio; (c) DSC thermogram of FV1 before and after immersion in water for 30 min; (d) DSC thermogram of HV1 before and after immersion in water for 30 min; (e) tensile test of FV1 after immersion in water for 0, 30 and 60 min (stretching rate 30 mm min^{-1}); (f) tensile test of HV1 after immersion in water for 0, 30 and 60 min (stretching rate 30 mm min^{-1}).

conducted on FV1 and HV1 after being immersed in water up to 1 h (Fig. 2e and f). Remarkably, FV1 showed no significant changes after immersion in water with its Young's modulus remaining mostly unchanged from 34.8 MPa to 33.8 MPa (3%) after 30 min and a slight decrease to 28.7 MPa (15%) was observed after 1 h of immersion. On the other hand, HV1 showed clear changes in its Young's modulus with a decrease from 2.18 MPa to 1.22 MPa (44%) after 30 min, and further to 0.74 MPa (66%) after 1 h of immersion. In addition, FTIR analysis of the samples also showed that the signals attributed to B–O–C and B–O were unaffected in FV1 after 1 h, which started decreasing at the 1.5 h mark, and only reduced significantly after 2 h of immersion; however, the signals in HV1 disappeared for HV1 after immersion in water for just 30 min (Fig. S23–S27, ESI†). These results indicate that the highly hydrophobic fluorinated side chains can successfully enhance the hydrolytic stability of boronic esters, which can be attributed to two possible mechanisms of protection, the first being the reduction of water absorbed into the matrix, the second being the repelling of water molecules in the matrix from approaching the boronic ester group. To clarify which mechanism has a higher effect, both FV1 and HV1 were swelled in water for 3 days to evaluate the water retention ability, which showed that despite FV1 absorbing more water than HV1 (Fig. S28, ESI†), FV1 still had a higher water-resistance than HV1, indicating that the enhanced hydrolytic stability effect was more likely to be due to the repelling of water molecules from the approaching boronic ester group.

To evaluate the effects of varying the proportion of hydrophobic side chains on the hydrolytic stability, two additional fluorinated vitrimers with increased ratios of 2,3-dihydroxypropyl acrylate and 2,2,2-trifluoroethyl acrylate were prepared. The vitrimer bearing a ratio of 30–70 was labelled FV2 and the one bearing a ratio of 40–60 was labelled FV3, which were both crosslinked to achieve a similar 10% overall crosslinking (Fig. S16, S29 and S30, ESI†). DSC and tensile tests were then conducted to evaluate the effect of decreased fluorinated side chains and increased free OH groups in the protection of the boronic ester linkages. As observed from the DSC results (Fig. S31 and S32, ESI†), after immersing FV2 in water for 30 min, there is a clear shift of the DSC curve with a drop of 7 °C for the T_g, while a more drastic shift was observed for FV3 with a drop of 11 °C for the T_g, indicating the counteracting effects of free OH groups in attracting H_2O being significant. Similar observations were made in the tensile tests of FV2 and FV3 after immersion in water (Fig. S33 and S34, ESI†), which showed a larger decrease in the Young's modulus with increasing free OH and reduced fluorinated side chain ratio. These results indicate a significant effect of the free –OH groups present, with increasing amounts of free –OH increasing the hydrophilicity of the material and reducing the efficiency of hydrophobic $–CF_3$ groups.

Utilizing the dynamic boronic ester network in FV1, it is capable of self-healing from damage in its bulk state *via* boronic ester exchange (Fig. 3a) and can also be mechanically and chemically recycled to prolong its usable service lifespan. To demonstrate its self-healing capabilities on a bulk scale (Fig. 3b), a 2 cm × 0.5 cm strip of FV1 was cut in half and joined back together and left to heal for 2 h. After healing for 2 h, the same piece of FV1 was able to be stretched to 225% of its original length before breaking, indicating a good degree of self-healing capabilities. Similarly on a microscopic scale (Fig. 3c), a 100 μm cut was made along the surface of a piece of 2 cm × 2 cm FV1 and left to heal over time, based on microscopic images at 20× magnification, it is observed that the inflicted cut could be closed after 1 h when left under ambient conditions. Subsequently, 1 cm × 0.5 cm samples of FV1 were cut in half and joined together and

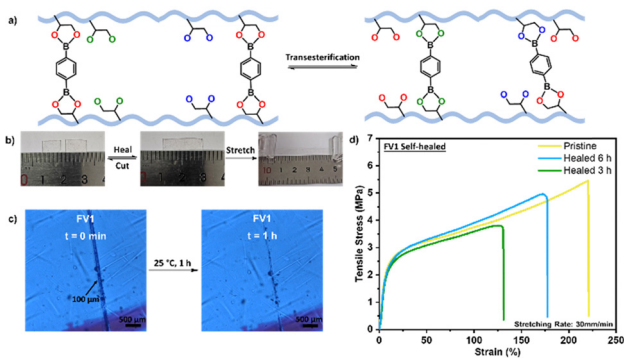

Fig. 3 Self-healing demonstration of FV1. (a) Mechanism of FV1 self-healing by boronic ester exchange; (b) strip of FV1 (2 × 0.5 cm) cut in two and joined to heal, and stretched to 225% of its original length (left to right); (c) microscopic images of FV1 at 0 min (left) and 1 h (right) after 100 μm damage was induced with a knife (20× magnification); (d) tensile testing of pristine and self-healed samples of FV1 at 3 h and 6 h.

left to heal for 3 h and 6 h, respectively. Tensile testing of these self-healed samples (Fig. 3d) showed a similar Young's modulus as a pristine sample of FV1, which shows a good degree of self-healing, albeit with a reduction in the maximum strain achieved.

To mechanically reprocess FV1, a sample of 2 g was cut into small pieces and mechanically pressed using a hot-press at room temperature and 20 bar for 15 min to reform a singular piece of FV1, with the duration reduced to 5 min when pressed at 100 °C (Fig. S35, ESI†). A similar 2 g sample could also be chemically recycled by the addition of methanol to redissolve the sample and heated to 60 °C for 4 h to reform the boronic ester network, yielding a pristine sample of FV1 after removal of methanol (Fig. S36, ESI†). FV1 can also be recycled into its linear polymer and crosslinker components using methanol and dialysis at room temperature. Upon stirring FV1 in a dialysis bag in methanol at room temperature for 24 h, FV1 can be separated into LP1 and 1,4-phenylenebisboronic acid. LP1 and 1,4-phenylenebisboronic acid recycled in this manner were characterized using ^{1}H NMR characterization (Fig. S37 and S38, ESI†) which showed no significant difference from the original counterparts. Similarly, when the recycled LP1 was also analysed using GPC (Fig. S39, ESI†) and DSC (Fig. S40, ESI†), the recycled LP1 gave similar results to the original. This method allows 87% recovery of LP1, which can be further fabricated into a new FV1 elastomer by the addition of 1,4-phenylenebisboronic acid as a crosslinker. The reprocessed and chemically recycled FV1 were analysed with FTIR and showed no significant deterioration from its pristine state (Fig. S41, ESI†). Tensile tests of the reprocessed and recycled FV1 also afforded similar stress–strain curves (Fig. S42, ESI†). The ease of recycling FV1 using simple methods and green solvents such as methanol further exemplifies its role as a circular material.

To conclude, we have designed and synthesized a boronic ester vitrimer with enhanced hydrolytic resistance by incorporating highly hydrophobic fluorinated side-chains into the polymer structure, which was able to maintain its thermal and mechanical properties in an RH 65% environment for 7 days and also demonstrated much slower degradation when immersed in water. Compared to the current state-of-the-art, this approach is simpler, more versatile, and achieves an outstanding waterproof performance. Besides, the utility of FV1 as a circular polymer was also demonstrated in its excellent reprocessability and recyclability, which can be achieved by multiple approaches of hot-pressing at room temperature for 15 min, redissolving in green solvents like methanol and ethanol, or recycling in methanol, with the resultant FV1 bearing no significant changes from the original. We believe that the enhanced hydrolytic resistance, along with the closed-loop reprocessability and recyclability of the boronic ester vitrimer presented in this work, holds great potential for the future development of robust, sustainable materials with a broader range of practical applications.

This project is supported by the Agency for Science, Technology and Research (A*STAR) under its RIE2025 Manufacturing, Trade and Connectivity (MTC) Programmatic Funding (Grant No. M22K9b0049).

Data availability

Data supporting the findings of this study are included in the article and its ESI.† Data are also available upon request.

Conflicts of interest

There are no conflicts to declare.

Notes and references

1 M. Qi, R. Yang, Z. Wang, Y. Liu, Q. Zhang, B. He, K. Li, Q. Yang, L. Wei, C. Pan and M. Chen, *Adv. Funct. Mater.*, 2023, **33**, 2214479.
2 H. Feng, S. Wang, J. Y. C. Lim, B. Li, W. Rusli, F. Liu, N. Hadjichristidis, Z. Li and J. Zhu, *Angew. Chem., Int. Ed.*, 2024, **63**, e202400955.
3 S. Wang, H. Feng, B. Li, J. Y. C. Lim, W. Rusli, J. Zhu, N. Hadjichristidis and Z. Li, *J. Am. Chem. Soc.*, 2024, **146**, 16112–16118.
4 P. Wang, L. Yang, B. Dai, Z. Yang, S. Guo, G. Gao, L. Xu, M. Sun, K. Yao and J. Zhu, *Eur. Polym. J.*, 2020, **123**, 109382.
5 M. Kathan, P. Kovaříček, C. Jurissek, A. Senf, A. Dallmann, A. F. Thünemann and S. Hecht, *Angew. Chem., Int. Ed.*, 2016, **55**, 13882–13886.
6 X. Li, R. Yu, Y. He, Y. Zhang, X. Yang, X. Zhao and W. Huang, *ACS Macro Lett.*, 2019, **8**, 1511–1516.
7 S.-M. Kim, H. Jeon, S.-H. Shin, S.-A. Park, J. Jegal, S. Y. Hwang, D. X. Oh and J. Park, *Adv. Mater.*, 2018, **30**, 1705145.
8 B. Zhou, T. Deng, C. Yang, M. Wang, H. Yan, Z. Yang, Z. Wang and Z. Xue, *Adv. Funct. Mater.*, 2023, **33**, 2212005.
9 H. Wang, Z. Shi, K. Guo, J. Wang, C. Gong, X. Xie and Z. Xue, *Macromolecules*, 2023, **56**, 2494–2504.
10 J. J. Q. Mah, K. Li, H. Feng, N. E. B. Surat'man, B. Li, X. Yu, M. Zhang, S. Wang and Z. Li, *Chem. – Asian J.*, 2024, **19**, e202400143.
11 J. J. Q. Mah, C.-G. Wang, N. Surat'man, S. F. D. Solco, A. Suwardi, S. Wang, X. J. Loh and Z. Li, *ACS Appl. Polym. Mater.*, 2023, **5**, 6747–6752.
12 S. Wang, N. Wang, D. Kai, B. Li, J. Wu, J. C. C. Yeo, X. Xu, J. Zhu, X. J. Loh, N. Hadjichristidis and Z. Li, *Nat. Commun.*, 2023, **14**, 1182.
13 Z.-H. Zhao, P.-C. Zhao, Y. Zhao, J.-L. Zuo and C.-H. Li, *Adv. Funct. Mater.*, 2022, **32**, 2201959.
14 A. Liguori and M. Hakkarainen, *Macromol. Rapid Commun.*, 2022, **43**, e2100816.
15 P. Chakma and D. Konkolewicz, *Angew. Chem., Int. Ed.*, 2019, **58**, 9682–9695.
16 X. Zhang, S. Wang, Z. Jiang, Y. Li and X. Jing, *J. Am. Chem. Soc.*, 2020, **142**, 21852–21860.
17 P. H. Kirchner, L. Schramm, S. Ivanova, K. Shoyama, F. Wurthner and F. Beuerle, *J. Am. Chem. Soc.*, 2024, **146**, 5305–5315.
18 M. Ma and W. Zhou, *Ind. Eng. Chem. Res.*, 2015, **54**, 2599–2605.
19 A. Höglund, M. Hakkarainen and A.-C. Albertsson, *Biomacromolecules*, 2010, **11**, 277–283.
20 B. Marco-Dufort, R. Iten and M. W. Tibbitt, *J. Am. Chem. Soc.*, 2020, **142**, 15371–15385.